VERSITA

OPTO-ELECTRONICS REVIEW **18**(1), 95–101

DOI: 10.2478/s11772-009-0025-8

Insight into precursor kinetics using an infrared gas analyser

K. KŁOS[1], A. PIOTROWSKI[1], W. GAWRON[*2], AND J. PIOTROWSKI[1]

[1]VIGO System SA, 129/133 Poznańska Str., 05-850 Ożarów Mazowiecki, Poland
[2]Institute of Applied Physics, Military University of Technology, 2 Kaliskiego Str., 00-908 Warsaw, Poland

Precursor kinetics and its influence on MOCVD growth was investigated using an infrared absorption gas analyser. After several refinements, the analyser was able to be used to measure time dependent concentrations of precursors in the growth zone. Changes were induced by periodic switching of corresponding bubbler valves. It was proved that precursor transport could be accurately described by the combined plug flow and perfectly mixed tank model. The studies of the precursor transport are strategically important for the growth of multilayer structures, when growth time of particular layers becomes comparable to delays and time constants. One example is quantum wells or interdiffused multilayer process (IMP) used in the growth of $Hg_{1-x}Cd_xTe$ heterostructures, where knowledge of precursor transport characteristics is vital for understanding and properly designing that growth. The model parameters, sc. the delays and time constants for DIPTe and DMCd, were evaluated for various growth conditions and then successfully used to optimise the growth of complex $Hg_{1-x}Cd_xTe$ heterostructures.

Keywords: $Hg_{1-x}Cd_xTe$, IR gas analyser, MOCVD.

1. Introduction

Usually, low volume and careful design of modern MOCVD reactors ensure that precursors transport and reactor residence times are short and negligible. Unfortunately there are some applications where growth time of particular layers becomes comparable to precursors transport and residence times. Such cases require precise quantification of precursor kinetics and transport and residence times must be known to control growth process. Examples are quantum wells or interdiffused multilayer process (IMP) used for growth of $Hg_{1-x}Cd_xTe$ heterostructures [1]. In this paper we focus on the latter, because in contrast to III-V materials mercury cadmium telluride (MCT) MOCVD manufacturers provide only equipment, without growth demonstration and the users must devise on their own suitable growth parameters. Stringent precursors control requirements for MCT growth are imposed by reactor design and IMP growth mode. Additional, asymmetric volumes of mercury zone placed before growth zone increase precursors transport and residence times. Simultaneously, IMP technique involves a careful balancing of flows and concentrations in order to create a uniform area on the substrate. Direct growth of $Hg_{1-x}Cd_xTe$ with uniform composition is difficult due to different reaction rates of the tellurium precursor for growing the mercury containing binary compared with cadmium-contained and inherent problem with doping. IMP overcomes this difficulty by alternate deposition of thin HgTe and CdTe films with independently optimised flow rates and precursors' concentrations. HgTe and CdTe binaries interdiffuse at growth temperature resulting in a bulk material of constant composition. Typical thickness of a single IMP cycle varies between 50–200 nm and depends on the layer composition due to large variations in the interdiffusion coefficient.

Practical devices need multilayer heterostructures with a uniform composition within each layer. This implies thin IMP pairs and short CdTe and HgTe growth phases. Practical consequence is that IMP growth phase times become comparable to the times required for precursor transport from bubblers to the growth zone. Other complications are different blanket flow rates for the CdTe and HgTe growth stages, synchronisation of precursors and dopants during the CdTe growth stage, and proper flush stages to prevent precursors from penetrating subsequent growth stages and unintentional growth at the interfaces. Poor precursors control may lead to growth conditions that adversely affect crystalline quality, homogeneity, and doping of the $Hg_{1-x}Cd_xTe$ layers.

Some preliminary results have been presented in Refs. 2 and 3. This paper details some of our recent work on the precursors' kinetics control and shows how IR gas analysers are suited for precursors kinetic measurements in quartz reactors.

2. System description

Experiments were carried out in AIX-200 system accommodated to MCT growth. It consisted of a horizontal rectangular duct quartz reactor cell (liner) enclosed in outer circu-

*e-mail: wgawron@wat.edu.pl

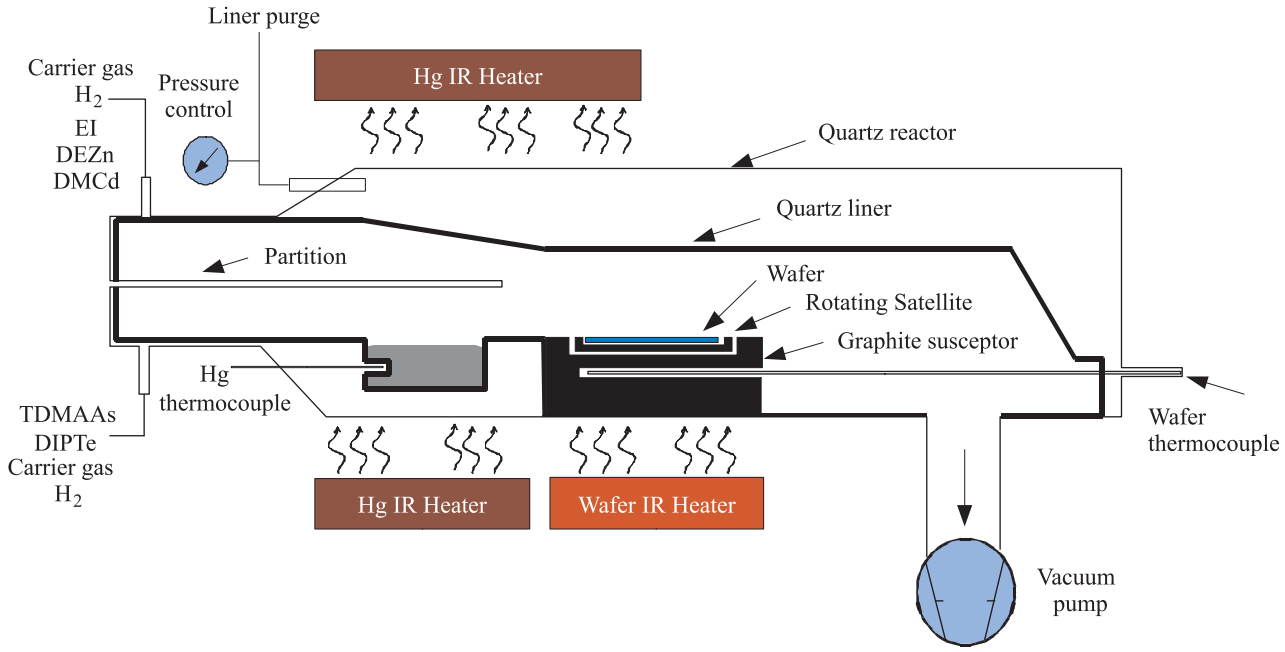

Fig. 1. Horizontal reactor cell with internal mercury source suitable for MCT growth.

lar quartz tube (Fig. 1). MCT reaction chambers tend to look quite different to their more conventional MOCVD counterparts, because they have a liquid mercury evaporation boat in the entrance zone of the reactor cell and separation of hydrogen carrier gas saturated with precursors to avoid premature reaction in Hg zone. The temperature of mercury was controlled by an external heater that also maintained control of the reactor cell ceiling temperature profile.

The wafer holder was made of SiC coated graphite capable of holding up to two-inch diameter substrate with gas foil rotation system. The substrate, GaAs (100)2°→(110) was heated with halogen heaters situated directly underneath the wafer holder.

The precursors, dimethylcadmium (DMCd), diisopropyltellurium (DIPTe) were adduct grade supplied by Epichem. The mercury source was a liquid mercury evaporation boat in the entrance zone of the reactor cell.

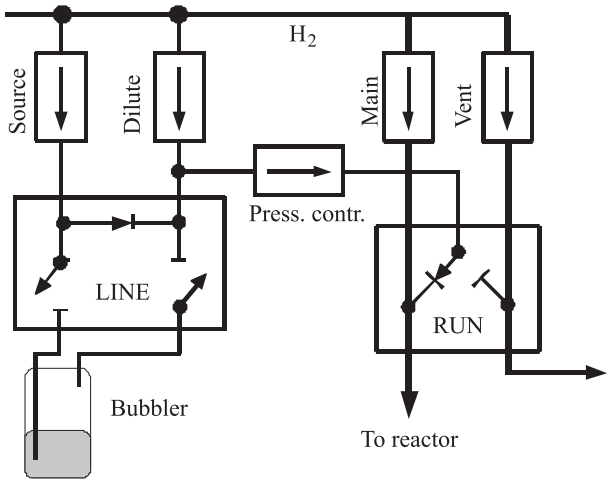

Fig. 2. Gas supply system in MOCVD.

Our MOCVD system does not have active pressure balancing between main and vent lines during switching RUN valve (Fig. 2). In connection with IMP mode growth, where ratio of flush times to growth times during one cycle varies from 30% to 100%, growth control through RUN valves would be very inefficient. Therefore, we decided to keep the RUN valve open and feeding precursors through the LINE valve. As a consequence of our approach, delivery times in LINE controlled injection are about two times longer and they are dependent on source flow through bubbler.

3. Precursor synchronization by CdTe growth experiments

Initially, we tried to synchronize DMCd and DIPTe precursors during CdTe growth phase. Relative transport times of DMCd and DIPTe were obtained from a series of CdTe growth runs. Experiments were set up as follows, periodically introduced 2 s pulses of DMCd and DIPTe followed by ~30 s of flush phase were grown. DMCd and DIPTe cycles were displaced by the "shift". The best synchronization of precursors' pulses in the growth zone gave the fastest growth rate and this thesis was confirmed by later measurements with IR analyser. Accuracy of synchronization quantification depends on a number of loops. Transmittance curves with interference peaks were used to measure the thickness of the deposited CdTe. Table 1 and Fig. 3 contain conditions and results of experiments.

Experiments 530–535 were conducted on single CdTe/GaAs heterostructure with transmittance measurements between growth runs. Subsequent buffer layer from 536 was used in 537 and 538. Cleaved samples of buffer from growth run 918 were used as substrate in 919–926 growth runs, which enable us to study influence of precursors synchroni-

Table 1. Conditions and results of CdTe growth runs. A minus sign indicates that DMCd was introduced before DIPTe, positive DIPTe before DMCd.

Growth nr.	Shift*, s	Precursors injection time, s	Cd/Te	Total Flow, lower/upper inlets, sccm	Loops	Thickness CdTe, nm	Growth rate, nm/s	Rq, nm
530	12.5	2	1.03	2000 + 500	720	1020	0.71	–
533	9.5	2	1.03	2000 + 500	720	1810	1.26	–
534	15.5	2	1.03	2000 + 500	720	580	0.40	–
535	6.5	2	1.03	2000 + 500	720	2165	1.50	–
536	0	900	1.03	2000 + 500	1	1305	1.45	–
537	3.5	2	1.03	2000 + 500	360	1000	1.39	–
539	8	2	1.03	2000 + 500	360	1055	1.47	–
590	0	1500	5.06	2000 + 500	1	620	0.41	–
591	0.75	2	5.06	2000 + 500	360	280	0.39	–
918	0	1290	1.03	1200 + 1200	1	1895	1.47	–
919	–2	2	1.03	1200 + 1200	300	960	1.60	11.2
920	0	2	1.03	1200 + 1200	200	305	0.76	15.8
923	–4	2	1.03	1200 + 1200	200	345	0.86	12.3
924	–1.5	2	1.03	1200 + 1200	150	370	1.23	7.4
925	–2	2	1.03	1200 + 1200	300	965	1.61	18.1
926	–1	2	5.06	1200 + 1200	300	180	0.30	29.8
927	0	5400	5.06	1200 + 1200	1	2175	0.40	–
928	0	5400	5.06	1200 + 1200	1	2435	0.45	–
929	–0.5	2	5.06	1200 + 1200	150	115	0.38	–
930	0	2	5.06	1200 + 1200	150	200	0.67	–
931	0.5	2	5.06	1200 + 1200	150	165	0.55	–

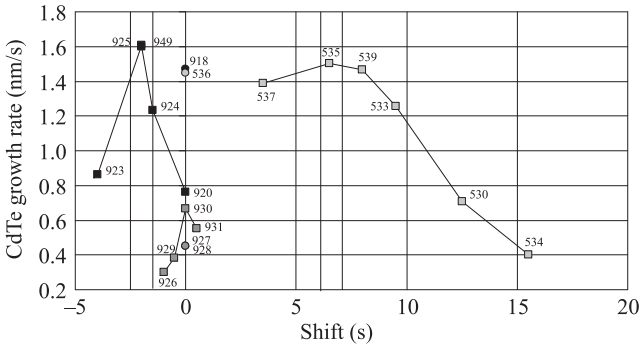

Fig. 3. Comparison of growth rate from continuous and pulsed depositions of CdTe, as a function of displacement of DMCd and DIPTe. Black points indicate experiments with 1.03 Cd/Te ratio and symmetrical total flow rate 1200 sccm + 1200 sccm through upper and lower inlet. Darkly grey points indicate experiments with 5.06 Cd/Te ratio and symmetrical total flow rate 1200 sccm + 1200 sccm through upper and lower inlet. Brightly grey points indicate experiments with 1.03 Cd/Te ratio and asymmetrical flow rate 2000 + 500 through upper and lower inlet, respectively. Spheres at 0 s shift represent growth rate from continuously deposited CdTe layers. Vertical lines illustrate best synchronization based on measurements with gas analyser at growth zone with ±0.5 s accuracy.

zation on morphology. Table 1 contains Rq measurement from a laser sccaterometer SL-31 based on total integrates scattering (TIS) and Fig. 4 shows Nomarsky photos of the measured samples. Buffers deposited with 5.06 Cd/Te ratio from 927 and 928 growth runs with deposited on them 929–931 experiments had morphologies out of scatterometer calibration.

Different flow velocities and volumes in corresponding parts of the gas system caused differences in DMCd and DIPTe transport times. Synchronization for flow 1200/1200 sccm with Cd/Te = 5.06 was obtained for DMCd and DIPTe LINE valves simultaneously opened. Changing Cd/Te to 1.03 caused a 2-s synchronization shift and for flow 2000/500 sccm precursors were synchronized when DMCd injection was retarded 6.5 s. Dull shape of the CdTe growth rate for asymmetric 2000 + 500 sccm carrier gas total flow rate is caused by large distortion of DIPTe concentration pulses during flow through vast space in a liner above mercury container. After these experiments, we decided to use symmetrical flow rate. This caused more compatible concentration changes of DMCd and DIPTe. Symmetrical carrier gas flow rate caused higher mercury loss with fast flow rate during CdTe growth phase.

Maximum growth rates obtained from pulsed mode were higher than the growth rate obtained by continuously

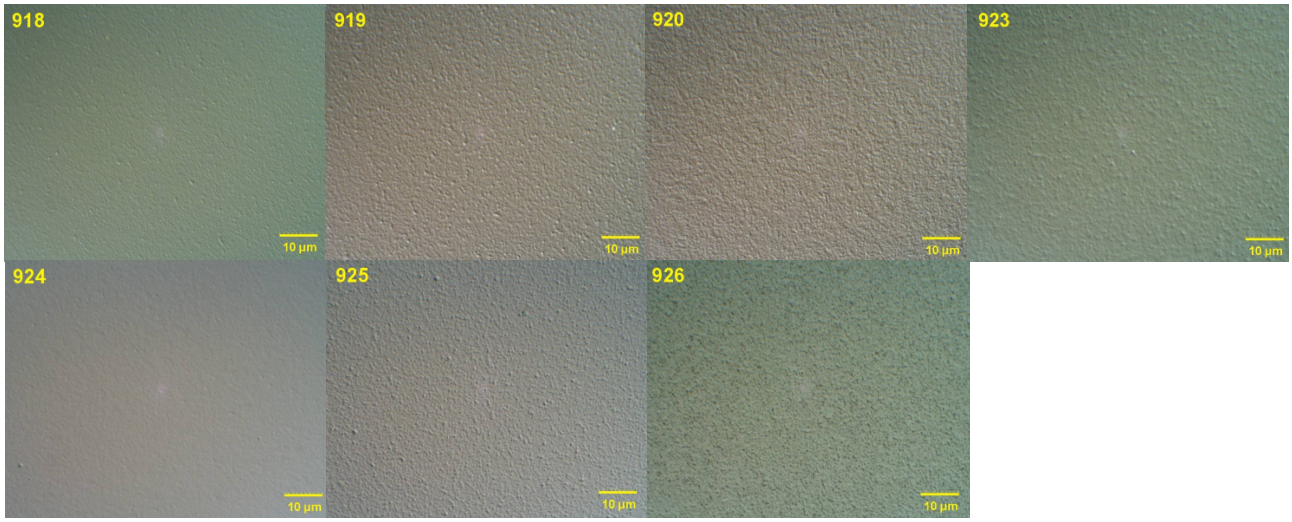

Fig. 4. Morphology of CdTe.

deposited buffer layers. This can be attributed to the influence of a prolonged nucleation stage or a less efficient saturation of carrier gas with precursors during continuously depositing CdTe in comparison to pulsed deposition.

Figure 4 contains Nomarsky pictures of CdTe morphology obtained during some of the growth experiments. CdTe from process 918 was cleaved and its pieces were used as a substrate in experiments 919–926. Among the processes with similar CdTe thickness 920–924, the best morphology was obtained for layer 924 where DMCd and DIPTe were almost synchronised.

Experiments with pulsed CdTe growth demonstrated the impact of growth conditions on precursor transport characteristics, but experiments are time consuming and the results obtained are relative ones.

4. Precursors' measurements with IR gas analyser

To obtain a better insight into the time dependent precursor transport characteristics of our system we applied in-situ monitoring of precursor concentration in the growth zone using an IR gas analyser (Fig. 5).

While developing the analyser, we had to overcome problems related to:

- adjusting gas analyser components in a hard to access, closely packed reactor cabinet,
- a small change in useful signal due to small absorption band of the MO compared to the incident radiation spectrum,
- fluctuations in the signal reference level caused by substrate and Hg heaters.

A schematic diagram of the gas analyser is depicted in Fig. 5. IR source radiation (halogen bulb) is collimated with the lens and passes through the reactor chamber. Then, the radiation is focused with the lens on the HgCdTe detector. A VIGO System narrow bandpass detector with a peak response at 3.4 µm was used.

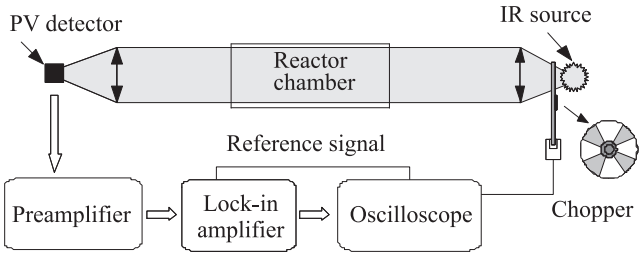

Fig. 5. Schematic of gas analyser.

We found that precursor concentration changes fit the model proposed by Svoronos, Woo, Irvine, Sankur, and Bajaj [4]. Precursor concentration changes in the growth zone can be described by a combination of two extreme conditions, plug flow (PF) and perfectly mixed tank (PMT). In the case of precursor plug flow, concentration is zero at the beginning of a growth stage and remains so until the time required to transport the precursors has elapsed when it steps up to a constant value. In the following flush phase concentration steps down to zero, but only after the precursors' transport time has elapsed. In the case of perfectly mixed tank conditions, concentration changes immediately after the precursor injection valve has been opened. The change in concentration can be described by an exponential function.

Precursor concentration changes in the growth zone can therefore be described by the combined model with two parameters, delay time and time constant.

The main level of insight into precursor kinetics is obtained with measurements of primary precursors at room temperature (Table 2, no. 1–3). These measurements provide model parameters corresponding to DIPTe concentration changes during the HgTe growth, flush phase and DIPTe and DMCd progress during the CdTe growth, flush phase.

The next level of insight into precursor kinetics required addressing the dependence of the precursor model parameters on growth zone and Hg zone temperature.

Table 2. Precursor measurement conditions with parameters obtained from fitting measured data to a combined model.

No.	Precursor	Distance	Temperature, Hg-zone/growth-zone, °C	Total Flow rate, upper + lower inlets, sccm	Source flow, sccm	Delay, s	Time const., s
1	DIPTe	Line valve – gr. zone	ambient/ambient	100 + 600	330	16.5	4
2	DIPTe	Line valve – gr. zone	ambient/ambient	1200 + 1200	330	10	2.3
3	DMCd	Line valve – gr. zone	ambient/ambient	1200 + 1200	37	12	3
4	DIPTe	Line valve – gr. zone	ambient/ambient	2000 + 500	330	18	3
5	DIPTe	Line valve – gr. zone	ambient/ambient	1200 + 1200	165	10.5	2.5
6	DMCd	Run/Vent valve – gr. zone	ambient/ambient	1200 + 1200	37	4.6	2.5
7	DMCd	Run/Vent valve – gr. zone	ambient/ambient	2000 + 500	37	4	2
8	DIPTe	Run/Vent valve – gr. zone	ambient/ambient	1200 + 1200	330	6.5	2
9	DIPTe	Line valve – gr. zone	ambient/200	1200 + 1200	330	9.5	2
10	DIPTe	Line valve – gr. zone	ambient/300	1200 + 1200	330	9.5	2
11	DIPTe	Line valve – gr. zone	200/ambient	1200 + 1200	330	10.3	2
12	DMCd	Line valve – gr. zone	ambient/200	1200 + 1200	37	11.5	2

The measurement of ambient temperature shown in Fig. 6 illustrates our problems with low frequency fluctuation of a reference level. We observed that increased temperature causes higher fluctuations and a lower signal from the precursor. We therefore employed the boxcar technique to obtain useful data. Comparing Fig. 6 measurements of DIPTe with those arranged in the same manner but in different growth zone temperatures reveals that temperature has little influence on delay time and none on time constants.

DMCd gives lower signals than DIPTe at the same concentrations which can be attributed to less absorbing bonds in the DMCd molecule. The DMCd measurements at 200°C on the left side of Fig. 7 are too distorted to extract reliable model parameters. The right side of Fig. 7 displays the measurements at the temperatures where pyrolysis occurs. Te molecules deposited on the liner give signals of one order of magnitude larger than DIPTe and screen accurate precursor concentration changes. Some of the Te evaporated during the pauses between precursor pulses but the signal did not reach reference level, and more Te was deposited on the liner after each pulse.

The measurements displayed in Fig. 8 prove that the model parameters are independent of Hg zone temperature. These results can be attributed to an adequate carrier gas flow rate and a low IR absorption coefficient for the carrier gas transporting the precursor.

5. Conclusions

This paper demonstrates that simple IR gas analyser measurements lend themselves well to the measuring parameters important for designing MCT process in the industrial MOCVD environment. The IR analyser measurements allow for better insight in precursor concentration changes in the reactor chamber which can help understand, design, and optimise IMP growth conditions. The obtained combined model parameters were used to design IMP processes

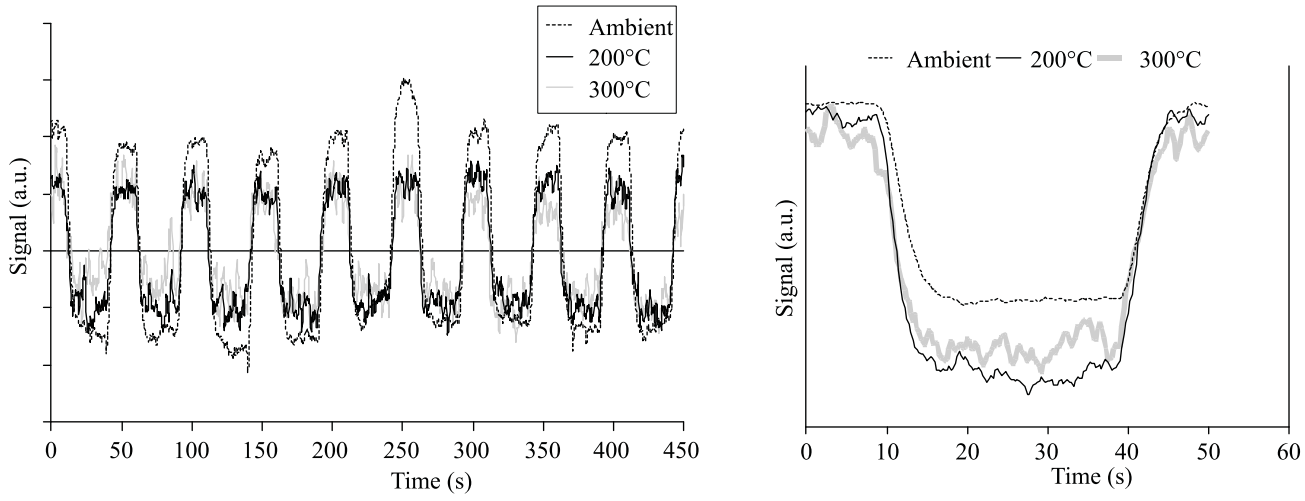

Fig. 6. Measurements 2, 9, and 10 from Table 2. Raw data (left side), boxcared (right side).

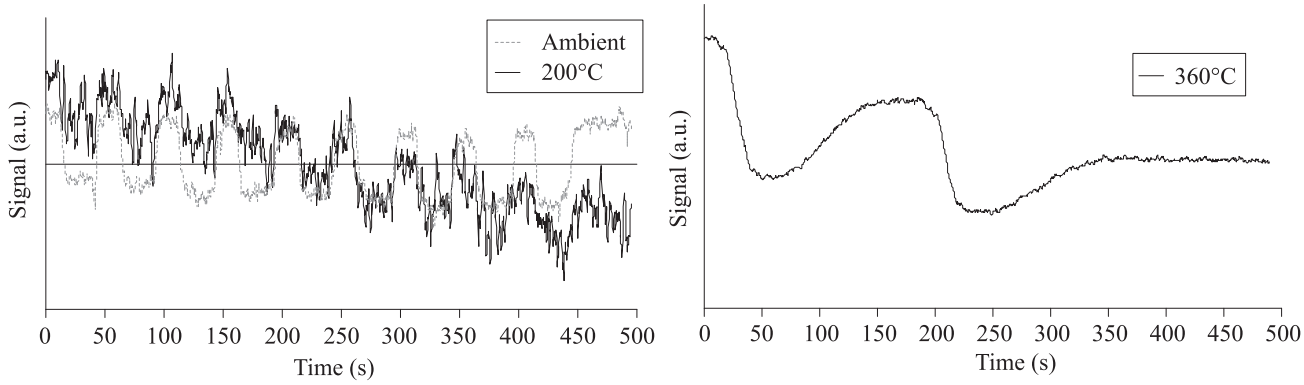

Fig. 7. Measurements of DMCd 3 and 12 from Table 2 (left side). Measurement of two DIPTe pulses at 360°C (right side).

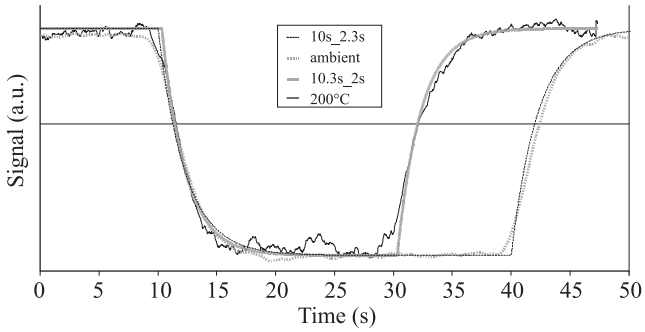

Fig. 8. Comparison of measurements 2 and 11 from Table 2 and their combined model fitting curves.

(Fig. 9) used in the processes which implement in situ stoichiometry control and enhanced dopant activation, and utilized in thousands heterostructures deposited by MOCVD laboratory in VIGO System S.A. [5–13].

Current IR analyser design provides time dependent measurements of the main precursors' concentration below their pyrolysis temperature. We are working to improve S/N of the analyser by replacing the monochrome PV detector with a multicoloured one and exchanging the halogen bulb for an IR LED.

Acknowledgements

This work was supported by the Polish Ministry of Science and Information Technology in the frame of project No. 0 T00A 010 30 and PBZ- MNiSW 02/I/2007.

References

1. J. Tunnicliffe, S.J.C. Irvine, O.D. Dosser, and J.B. Mullin, "A new MOVPE technique for the growth of highly uniform CMT", *J. Cryst. Growth* **68**, 245–253 (1984).
2. A. Piotrowski, P. Madejczyk, W. Gawron, K. Kłos, J. Pawluczyk, M. Grudzień, J. Piotrowski, and A. Rogalski, "Recent progress in MOCVD growth of $Hg_{1-x}Cd_xTe$ heterostructures for uncooled infrared photodetectors", *Proc. SPIE* **5957**, 273–284 (2005).
3. A. Piotrowski and K. Kłos, "Metal-organic chemical vapour deposition of HgCdTe fully doped heterostructures without post-growth anneal for uncooled MWIR and LWIR detectors", *J. Electron. Mater.* **36**, 1052–1058 (2007).
4. S.A. Svoronos, W.W. Woo, S.J.C. Irvine, H.O. Sankur, and J. Bajaj, "A model of the interdiffused multilayer process", *J. Electron. Mater.* **25**, 1561–1571 (1996).
5. www.vigo.com.pl.
6. A. Piotrowski, P. Madejczyk, W. Gawron, K. Kłos, J. Pawluczyk, M. Grudzień, J. Piotrowski, and A. Rogalski, "Growth of MOCVD HgCdTe heterostructures for uncooled

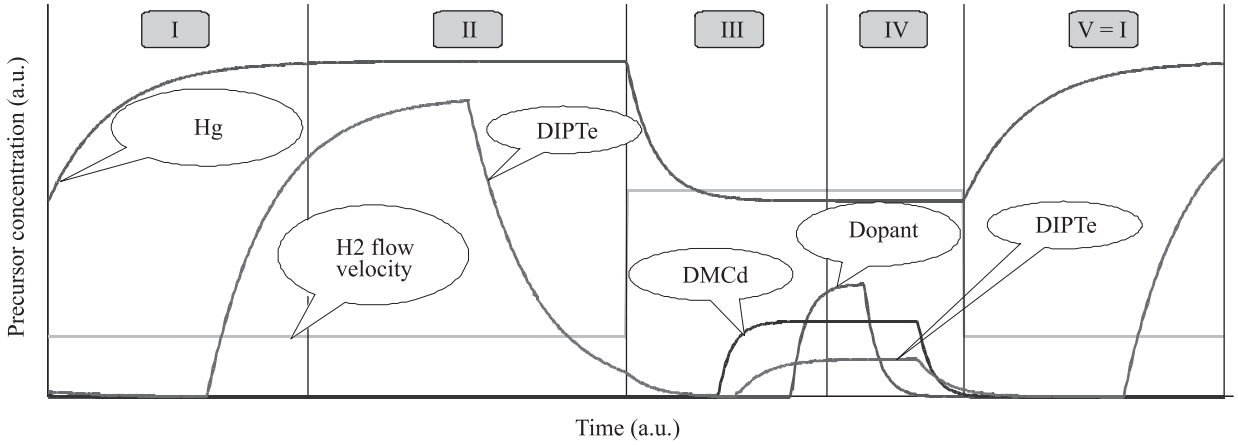

Fig. 9. Scheme of precursors and flow changes during typical doped IMP period. Dopant and Hg concentration off-scale. I-HgTe growth stage, II-HgTe flush stage, III-CdTe growth stage, IV-CdTe flush stage, V-HgTe growth stage of next IMP period.

infrared photo detectors", *B. Pol. Acad. Sci-Te.* **53**, 139–149 (2005).
7. P. Madejczyk, A. Piotrowski, W. Gawron, K. Kłos, J. Pawluczyk, J. Rutkowski, J. Piotrowski, and A. Rogalski, "Growth and properties of MOCVD HgCdTe epilayers on GaAs substrates", *Opto-Electron. Rev.* **13**, 239–251 (2005).
8. W. Gawron, M. Grudzień, K. Kłos, A. Piotrowski, and J. Piotrowski, "Investigations of HgCdTe growth with MOCVD method at VIGO-MUT laboratory", *Elektronika* **3**, 14–19 (2006). (in Polish)
9. A. Piotrowski, P. Madejczyk, W. Gawron, K. Kłos J. Pawluczyk, J. Rutkowski, J. Piotrowski, and A. Rogalski, "Progress in MOCVD growth of HgCdTe heterostructures for uncooled infrared photodetectors", *Infrared Phys. Techn.* **49**, 173–182 (2007).
10. A. Piotrowski, K. Kłos, W. Gawron, J. Pawluczyk, Z. Orman, and J. Piotrowski, "Uncooled or minimally cooled 10-μm photodetectors with subnanosecond response time", *Proc. SPIE* **6542**, 0277786X (2007).
11. A. Piotrowski, K. Kłos, W. Gawron, J. Pawluczyk, Z. Orman, and J. Piotrowski, "Uncooled or minimally cooled 10-μm photodetectors with subnanosecond response time", *Proc. SPIE* **6542**, 0277786X (2007).
12. A. Piotrowski, W. Gawron, K. Kłos, J. Rutkowski, Z. Orman, J. Pawluczyk, D. Stanaszek, H. Mucha, J. Piotrowski, and A. Rogalski, "New generation uncooled and minimally cooled detectors of medium and far IR", *Elektronika* **11**, 112–121 (2008).
13. J. Rutkowski, P. Madejczyk, A. Piotrowski, W. Gawron, K. Jóźwikowski, and A. Rogalski, "Two-colour HgCdTe infrared detectors operating above 200 K", *Opto-Electron. Rev*. **16**, 321–327 (2008).